Single-Molecule Vibrational Spectroscopy and Microscopy

Single-Molecule Vibrational Spectroscopy and Microscopy

B. C. Stipe, M. A. Rezaei, W. Ho*

Vibrational spectra for a single molecule adsorbed on a solid surface have been obtained with a scanning tunneling microscope (STM). Inelastic electron tunneling spectra for an isolated acetylene (C_2H_2) molecule adsorbed on the copper (100) surface showed an increase in the tunneling conductance at 358 millivolts, resulting from excitation of the C-H stretch mode. An isotopic shift to 266 millivolts was observed for deuterated acetylene (C_2D_2). Vibrational microscopy from spatial imaging of the inelastic tunneling channels yielded additional data to further distinguish and characterize the two isotopes. Single-molecule vibrational analysis should lead to better understanding and control of surface chemistry at the atomic level.

Vibrational spectroscopy is a powerful tool for the analysis of molecules adsorbed on surfaces. Knowledge of the active vibrational modes of a molecule, as well as the vibrational energies, can lead to an understanding of its adsorption site, orientation, and changes in bonding upon adsorption. This understanding is necessary for the elucidation of surface phenomena and for technologically important processes such as heterogeneous catalysis and epitaxial growth. Vibrational spectra are also "fingerprints" of adsorbed molecules and can be used for chemical identification.

In 1966 it was discovered that vibrational spectra can be obtained from molecules adsorbed at the buried metal-oxide interface of a metal-oxide-metal tunneling junction (1). In that experiment, the tunneling current I was measured as a function of voltage V across the junction. Small, sharp increases in the ac tunneling conductance, dI/dV, were observed when the energy of the tunneling electrons reached the energy of a vibrational mode for molecules in the junction. This increase is the result of electrons losing their energies to the vibrational mode, giving rise to an inelastic tunneling channel, which is forbidden when tunneling electrons have energies below the quantized vibrational energy. In the experiment, a peak at each vibrational energy was observed in d^2I/dV^2. This method, known as inelastic electron tunneling spectroscopy (IETS), has been applied to a wide range of systems and has led to a better understanding of molecules in the adsorbed state (2). However, IETS has a major drawback: Molecules are buried within the junction in a complex environment that is difficult to characterize. For this reason, IETS is not as broadly applicable as electron energy loss

spectroscopy (EELS) and infrared spectroscopy, which can be performed on exposed, well-ordered surfaces in ultrahigh vacuum (UHV). However, IETS is about 10 times as sensitive as these other techniques (3); as few as 10^9 molecules are needed within the junction to give a useful spectrum (4).

Here, we used a UHV scanning tunneling microscope (STM) to extend the IETS method to a single molecule. In this arrangement, the metal-oxide-metal tunnel junction is replaced by the STM tunnel junction: a sharp metal tip, a vacuum gap of several angstroms, and a surface with the adsorbed molecules. The STM is capable of imaging surfaces with atomic resolution, and therefore the molecule's bonding environment with respect to an ordered surface can be determined precisely. By probing individual molecules, it should be possible to explore how vibrational properties are affected by neighboring coadsorbed species or surface defects. It is widely believed that such local effects play a critical role in surface chemistry. The combination of atomic resolution and vibrational spectroscopy also allows the creation of atomic-scale spatial images of the inelastic tunneling channel for each vibrational mode, in a manner similar to that used to map out the electronic density of states with the STM (5). Thus, individual adsorbed molecules can be identified by their vibrational spectra and inelastic images. In contrast, identification and characterization by electronic spectroscopy is problematic for two reasons: considerable broadening and shifting of the electronic energy levels occurs upon adsorption, and the adsorbed molecule's spectrum becomes convolved with the STM tip's electronic spectrum.

The possibility of vibrational spectroscopy with the STM was apparent soon after its invention. Theoretical estimates of the maximum changes in the ac conductance across the vibrational excitations ranged

Laboratory of Atomic and Solid State Physics and Center for Materials Research, Cornell University, Ithaca, NY 14853, USA.

*To whom correspondence should be addressed. E-mail: wilsonho@msc.cornell.edu

from 1 to 10% (6–9). An experiment probing the ac conductance over a cluster of sorbic molecules on graphite at 4 K reported extremely large (up to 1000%) jumps, which were attributed to characteristic vibrations of the molecules (10). However, no reproducible spectra were obtained because of diffusion events (molecules jumping) during the experiment. It is also possible that these diffusion events were responsible for some of the spectral features seen. In another experiment, a microscopic tunnel junction was created by adjusting the pressure between two crossed wires coated with a thin film (11). Two peaks were observed in d^2I/dV^2 at bias voltages of 359 and 173 mV; these were assigned to the C-H stretch and bending vibrations of hydrocarbon contaminants, respectively. These results demonstrated that IETS could be achieved in a microscopic tunneling junction. Vibrational spectroscopy with the STM has proved difficult because of the extreme mechanical stability necessary to observe small changes in tunneling conductance. For example, the physics of tunneling dictates a tunneling gap stability of ~0.01 Å to keep the conductance stable to within 2%.

Details of our homemade STM and experimental setup have been described elsewhere (12). The STM tip and Cu(100) sample were prepared and cooled to 8 K (13). The surface was dosed with acetylene until a coverage of ~0.001 monolayer was observed on the surface with the STM. If desired, the surface was subsequently dosed with deuterated acetylene to the same coverage. Although the identity of the isotopes was known by comparing images before and after each dose, they were not distinguishable in the constant-current STM images.

A definitive determination of the adsorption site and orientation of acetylene on Cu(100) has not been reported to date, although the C-C bond is known to be parallel to the surface (14). Considerable rehybridization of the molecule occurs upon adsorption, leading to a lengthening of the C-C bond (14) and a concomitant tilting of the C-H bond away from the surface (15). The atomically resolved STM images (Fig. 1) indicate that the molecule is adsorbed on the hollow sites of the surface, with the plane of the molecule across the diagonal of the square formed by four Cu atoms. This is consistent with one of two proposed adsorption sites, as determined from EELS data (16), and with the proposed site for acetylene on Ni(100) (17). There are two equivalent adsorption sites rotated 90° from each other. The reversible rotation of the molecule between these two orientations can be induced by the tunneling current. Therefore, it is desirable to position the tip over
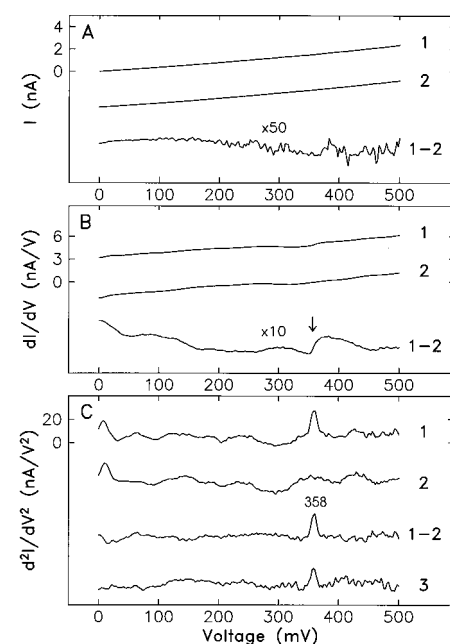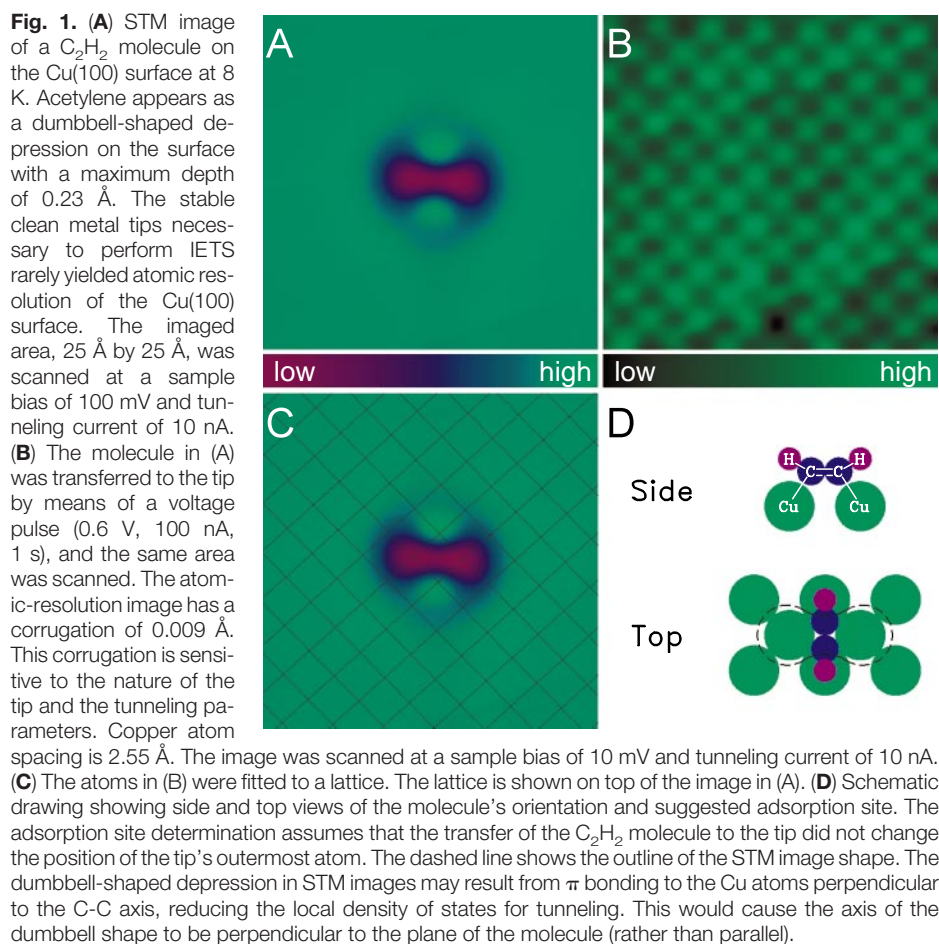
the center of the adsorbed molecule so that the rotational motion does not affect the tunneling current in the recording of the vibrational spectra.

In IETS, changes in the ac conductance, $\sigma = dI/dV$, appear at characteristic tunneling voltages (V_v, defined as vibrational voltages) such that $eV_v = h\nu$, where e is the charge of the electron, h is the Planck constant, and ν is the vibrational frequency. Vibrational spectra were obtained with the use of an iterative tracking scheme to position the tungsten tip at the center of the molecule, with lateral and vertical resolutions of better than 0.1 and 0.01 Å, respectively. This was done by locating a local minimum of the tip height with the STM's feedback loop turned on to maintain constant tunneling current. For sharp tips, this minimum did not occur at the center of the molecule; offsets were added to position the tip in these cases. Tracking of the symmetry point of acetylene was carried out at a sample bias of 250 mV and tunneling current of 1 nA. Feedback was then turned off. The tip remained stationary while the vibrational spectrum was recorded. A sinusoidal modulation at 200 Hz and 2 to 20 mV rms amplitude was added to the dc sample bias voltage. The tunneling current was fed into a lock-in amplifier to determine the first and second harmonics of the modulation frequency (these are proportional to dI/dV and d^2I/dV^2, respectively). These signals were recorded as the sample bias voltage was swept from 0 to 500 mV and back down to 0 mV in ~2 min (18). After each triangular sweep of the bias voltage, feedback was turned on to allow automatic tracking of the molecule before the next sweep. Spectra were averaged after each pass, although the C-H (and C-D) stretch peak in d^2I/dV^2 was usually distinguishable from the background after a single sweep. The noise level of the tunneling current during these experiments was measured to be ~25 fA Hz$^{-1/2}$ at 1 nA, which is close to the theoretical shot noise limit of 18 fA Hz$^{-1/2}$ at this current. The I-V curves were measured separately.

In addition to the spectra obtained over the symmetry point of a molecule, spectra were also recorded over a clean area of the surface by displacing the tip by ~20 Å. Contributions from the electronic spectrum of the tip and substrate can be minimized by subtracting the clean spectra from the molecular spectra. The I-V curves for a single C_2H_2 molecule and the clean surface (Fig. 2A) show the expected linear dependence for metallic junctions. An increase of 4.2% in dI/dV at the vibrational voltage can be seen in the difference spectrum (Fig. 2B). The d^2I/dV^2 spectrum taken over the molecule reveals a distinct peak at 358 mV (Fig. 2C). In addition to enhancing the signal-to-noise ratio, the long signal average time of 10 hours over the symmetry point of a single molecule at 2 mV modulation (line 3 in Fig. 2C) demonstrates the stability of the experiment. Here, a different tip was used that gave an increase of 3.3% in the ac conductance. The size of the peak was found to be tip dependent, with sharper tips (as determined from the resolution in the STM images) giving larger vibrational peaks. A change in ac conductance across

Fig. 2. (**A**) *I-V* curves recorded with the STM tip directly over the center of molecule (1) and over the bare copper surface (2). The difference curve (1 − 2) shows little structure. Each scan took 10 s. (**B**) *dI/dV* from the lock-in amplifier recorded directly over the center of the molecule (1) and over the bare surface (2). The difference spectrum (1 − 2) shows a sharp increase at a sample bias of 358 mV (arrow). Spectra are the average of 25 scans of 2 min each. A sample bias modulation of 5 mV was used. (**C**) *d²I/dV²* recorded at the same time as the data in (B) directly over the molecule (1) and over the bare surface (2). The difference spectrum shows a peak at 358 mV. The area of the peak gives the conductance change, Δσ (Δσ/σ = 4.2%). A difference spectrum taken with 2 mV modulation and a different tip (3) shows a smaller peak (Δσ/σ = 3.3%). The data in (3) are the result of an average of 279 scans of 2 min each (10 hours total scanning time directly over the molecule). Data in (B) were calibrated by numerical integration and comparison with the data in (A). Data in (C) were calibrated by numerical integration and comparison with the calibrated data from (B).

Fig. 1. (**A**) STM image of a C_2H_2 molecule on the Cu(100) surface at 8 K. Acetylene appears as a dumbbell-shaped depression on the surface with a maximum depth of 0.23 Å. The stable clean metal tips necessary to perform IETS rarely yielded atomic resolution of the Cu(100) surface. The imaged area, 25 Å by 25 Å, was scanned at a sample bias of 100 mV and tunneling current of 10 nA. (**B**) The molecule in (A) was transferred to the tip by means of a voltage pulse (0.6 V, 100 nA, 1 s), and the same area was scanned. The atomic-resolution image has a corrugation of 0.009 Å. This corrugation is sensitive to the nature of the tip and the tunneling parameters. Copper atom spacing is 2.55 Å. The image was scanned at a sample bias of 10 mV and tunneling current of 10 nA. (**C**) The atoms in (B) were fitted to a lattice. The lattice is shown on top of the image in (A). (**D**) Schematic drawing showing side and top views of the molecule's orientation and suggested adsorption site. The adsorption site determination assumes that the transfer of the C_2H_2 molecule to the tip did not change the position of the tip's outermost atom. The dashed line shows the outline of the STM image shape. The dumbbell-shaped depression in STM images may result from π bonding to the Cu atoms perpendicular to the C-C axis, reducing the local density of states for tunneling. This would cause the axis of the dumbbell shape to be perpendicular to the plane of the molecule (rather than parallel).

1733

the C-H peak of 11.8% was measured for one sharp tip. The peak was observed for every tip used, and spectra were reproducible for a given tip. The peak position remained the same to within 1 mV even when the tunneling current was increased by a factor of 10. Spectra measured with negative bias voltages showed the expected negative peak at −358 mV. Therefore, no electric field–dependent peak shifts have been measured.

The full width at half maximum (FWHM) of the d^2I/dV^2 vibrational peak is given by $V = [(1.7V_m)^2 + (5.4kT/e)^2 + W^2]^{1/2}$, where V_m is the modulation voltage, k is the Boltzmann constant, T is temperature, and W is the intrinsic width (2). Typical values of the FWHM for the 358-mV peak obtained at modulation voltages of 20, 10, 5, and 2 mV are 34, 17, 12, and 10 mV, respectively. Comparison with the above formula suggests an intrinsic width of
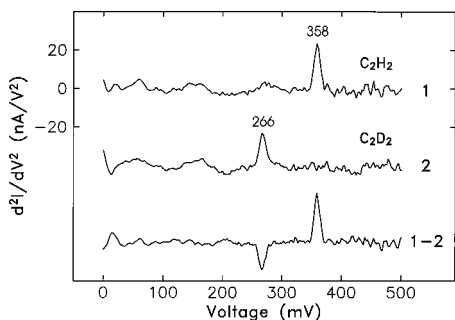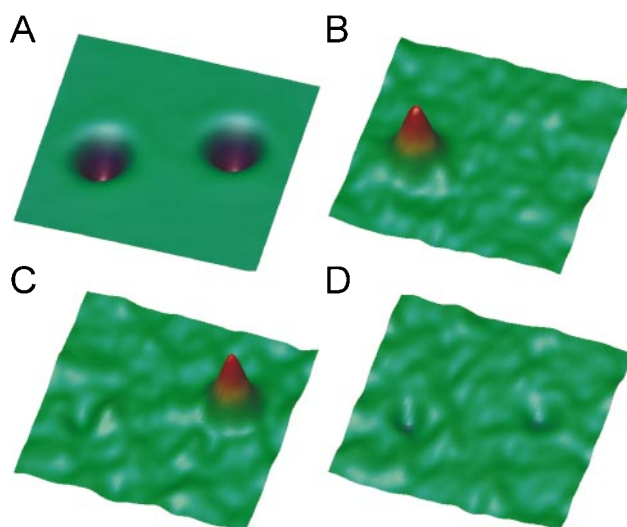

Fig. 3. Background difference d^2I/dV^2 spectra for C_2H_2 (1) and C_2D_2 (2), taken with the same STM tip, show peaks at 358 mV and 266 mV, respectively. The difference spectrum (1 − 2) yields a more complete background subtraction. For this tip, $\Delta\sigma/\sigma = 6.2\%$ and 4.5% for C_2H_2 and C_2D_2, respectively.

~8 mV, larger than is typically seen in macroscopic IETS.

Isotopic substitution is a powerful tool for vibrational analysis. The C-H stretch at 358 mV was observed to shift to 266 mV for C_2D_2 (Fig. 3). These values are in close agreement with those obtained by EELS: 357, 360, and 362 meV for the C-H stretch of C_2H_2 on Cu(100) (16), Cu(110) (19), and Cu(111) (20), respectively; 272 and 270 meV for the C-D stretch of C_2D_2 on Cu(110) (19) and Cu(111) (20), respectively. Changes in ac tunneling conductance were typically ~30% lower for the C-D stretch relative to the C-H stretch. Other vibrational modes of adsorbed acetylene, such as the bending modes, were not observed. The prominence of the C-H stretch mode has also been observed in the macroscopic (1, 2) and microscopic (11) IETS measurements.

The ability to spectroscopically identify molecules with the STM makes it possible to implement chemically sensitive microscopy. Vibrational imaging of the adsorbed molecule was obtained while scanning the tip in constant-current mode to record the surface topography. At each data point, the feedback was turned off and the bias modulation turned on to record dI/dV and d^2I/dV^2. This procedure resulted in three images of the same area. As expected, no contrast was observed in a constant-current image of both acetylene isotopes (Fig. 4A). When the dc bias voltage was fixed at 358 mV, only one of the two molecules was revealed in the image constructed from the d^2I/dV^2 signal (Fig. 4B). By changing the dc bias voltage to 266 mV, the other molecule was imaged (Fig. 4C). Two small identical depressions observed at 311 mV (Fig. 4D) were attributed to the

change in the electronic density of states on the sites of the two molecules. The spatial extent of the inelastic tunneling channels appears to be at least as narrow as the constant-current molecular image.

For sharp tips, values of $\Delta\sigma/\sigma$ of up to 12% and 9% have been measured for the C-H and C-D stretch peaks, respectively. This is considerably larger than the values obtained in conventional IETS. The dipole scattering approximation usually used to model IETS spectra yielded theoretical estimates of $\Delta\sigma/\sigma$ in STM-IETS on the order of 1% (6, 7). It has been suggested, however, that the dipole scattering approximation may not be valid for the molecular-sized tunneling gaps in the STM, and that resonance and impact scattering may lead to enhancement in $\Delta\sigma/\sigma$ by a factor of ~10 (8, 9). The size of the observed peaks, the spatial extent of the inelastic channels, and the strong tip dependence are consistent with the resonance scattering mechanism. The relatively large intrinsic peak width may also be a result of the resonant tunneling mechanism.

Vibrational spectroscopy at the single-molecule level opens new avenues of research, both experimental and theoretical. The extension of our work to other functional groups should allow the characterization of small molecules in more complex environments, as well as the analysis of larger molecules of chemical and biological interest. It may soon be possible to use single-molecule vibrational spectroscopy and microscopy to determine the identity and arrangement of functional groups within a single molecule and to study its chemical transformation.

REFERENCES AND NOTES

1. R. C. Jaklevic and J. Lambe, *Phys. Rev. Lett.* **17**, 1139 (1966).
2. P. K. Hansma, *Phys. Rep.* **30C**, 145 (1977); W. H. Weinberg, *Annu. Rev. Phys. Chem.* **29**, 115 (1978); T. Wolfram, Ed., *Inelastic Electron Tunneling Spectroscopy* (Springer-Verlag, Berlin, 1978); P. K. Hansma, Ed., *Tunneling Spectroscopy* (Plenum, New York, 1982).
3. H. Ibach and D. L. Mills, *Electron Energy Loss Spectroscopy* (Academic Press, New York, 1982).
4. R. M. Kroeker and P. K. Hansma, *Surf. Sci.* **67**, 362 (1977).
5. R. J. Hammers, R. M. Tromp, J. E. Demuth, *Phys. Rev. Lett.* **56**, 1972 (1986).
6. G. Binnig, N. Garcia, H. Rohrer, *Phys. Rev. B* **32**, 1336 (1985).
7. B. N. J. Persson and J. E. Demuth, *Solid State Commun.* **57**, 769 (1986).
8. B. N. J. Persson and A. Baratoff, *Phys. Rev. Lett.* **59**, 339 (1987).
9. M. A. Gata and P. R. Antoniewicz, *Phys. Rev. B* **47**, 13797 (1993).
10. D. P. E. Smith, M. D. Kirk, C. F. Quate, *J. Chem. Phys.* **86**, 6034 (1987).
11. S. Gregory, *Phys. Rev. Lett.* **64**, 689 (1990).
12. B. C. Stipe, M. A. Rezaei, W. Ho, *J. Chem. Phys.* **107**, 6443 (1997). The variable-temperature STM and the sample are in thermal equilibrium inside a double copper housing cooled by a continuously

Fig. 4. Spectroscopic spatial imaging of the inelastic channels for C_2H_2 and C_2D_2. (**A**) Regular (constant current) STM image of a C_2H_2 molecule (left) and a C_2D_2 molecule (right). Data are the average of the STM images recorded simultaneously with the vibrational images. The imaged area is 48 Å by 48 Å. d^2I/dV^2 images of the same area recorded at (**B**) 358 mV, (**C**) 266 mV, and (**D**) 311 mV are the average of four scans of 25 min each with a bias modulation of 10 mV. All images were scanned at

1 nA dc tunneling current. The symmetric, round appearance of the images is attributable to the rotation of the molecule between two equivalent orientations during the experiment.

flowing liquid He cryostat. Thermal stability of the STM and the sample to within 0.01 K was reached 4 hours after initial cooling from room temperature.

13. Tips were made by etching polycrystalline tungsten wire in KOH. Tips were cleaned in UHV by repeated cycles of sputtering from field emission in a Ne atmosphere and annealing with an electron beam heater. Tips were sharpened just before the experiment by bringing the end of the tip in contact with the clean copper surface. Thus, the last atom on the tip is likely to be copper rather than tungsten. Cu(100) was cleaned with repeated cycles of 1 keV Ne$^+$ sputtering and annealing at 500°C until large defect-free regions of the surface were observed with the STM.

14. D. Arvanitis, U. Dobler, L. Wenzel, K. Baberschke, J. Stohr, *Surf. Sci.* **178**, 686 (1986).

15. X. F. Hu, C. J. Chen, J. C. Tang, *ibid.* **365**, 319 (1996).

16. Ts. S. Marinova and P. K. Stefanov, *ibid.* **191**, 66 (1987).

17. N. Sheppard, *J. Electron Spectrosc. Relat. Phenom.* **38**, 175 (1986).

18. Drifts were generally negligible during the time of each voltage sweep. With the feedback off, drift rates of ~0.001 Å min^{-1} and 0.01 Å min^{-1} were measured in the vertical and horizontal directions, respectively. By averaging spectra in the forward and backward sweep directions, the resulting small drift in the tunneling conductance was canceled out.

19. N. R. Avery, *J. Am. Chem. Soc.* **107**, 6711 (1985).

20. B. J. Bandy, M. A. Chesters, M. E. Pemble, G. S. McDougall, N. Sheppard, *Surf. Sci.* **139**, 87 (1984).

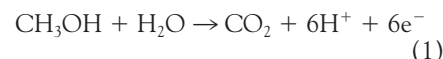21. Supported by NSF grant DMR-9707195.

Combinatorial Electrochemistry: A Highly Parallel, Optical Screening Method for Discovery of Better Electrocatalysts

Erik Reddington, Anthony Sapienza, Bogdan Gurau, Rameshkrishnan Viswanathan, S. Sarangapani, Eugene S. Smotkin,* Thomas E. Mallouk*

Combinatorial screening of electrochemical catalysts by current-voltage methods can be unwieldy for large sample sizes. By converting the ions generated in an electrochemical half-cell reaction to a fluorescence signal, the most active compositions in a large electrode array have been identified. A fluorescent acid-base indicator was used to image high concentrations of hydrogen ions, which were generated in the electrooxidation of methanol. A 645-member electrode array containing five elements (platinum, ruthenium, osmium, iridium, and rhodium), 80 binary, 280 ternary, and 280 quaternary combinations was screened to identify the most active regions of phase space. Subsequent "zoom" screens pinpointed several very active compositions, some in ternary and quaternary regions that were bounded by rather inactive binaries. The best catalyst, platinum(44)/ruthenium(41)/osmium(10)/iridium(5) (numbers in parentheses are atomic percent), was significantly more active than platinum(50)/ruthenium(50) in a direct methanol fuel cell operating at 60°C, even though the latter catalyst had about twice the surface area of the former.

Combinatorial synthesis and analysis have become commonly used tools in bioorganic chemistry (*1–11*). Although the combinatorial (or multiple sample) approach to the discovery of inorganic materials has existed for more than two decades (*12*), new materials (*13, 14*) and sensors (*15*) only recently have been discovered by this advanced Edisonian technique. There are several examples of combinatorial searches that have confirmed the properties of known materials (*16, 17*) and catalysts (*18*). There are, however, no previous reports of superior catalysts that have been identified by combinatorial chemistry. Combinatorial searches for catalysts are often limited not by synthesis but by the lack of methods that can simultaneously screen many composi-

tions. Recently, significant progress has been made in the thermographic screening of catalysts (*18, 19*). We describe here a general combinatorial screening method for electrode materials and its application to the problem of anode catalysis in direct methanol fuel cells (DMFCs). By screening combinations of five elements (Pt, Ru, Os, Ir, and Rh), we found several good catalysts in unexpected regions of composition space and identified a quaternary catalyst with significantly higher activity than the best previously known catalyst (a binary Pt-Ru alloy).

Because methanol is a renewable liquid fuel, DMFCs present some distinct potential advantages over combustion engines and hydrogen fuel cells for transportation and remote power applications. They are silent and nonpolluting, and they use an easily distributed, high-energy-density fuel (*20*). One of the factors that limits their development and use is that known anode and cathode electrocatalysts produce useful current densities only at high overpotentials. The anode catalyst is particularly problematic, because it must perform a ki-

netically demanding reaction, the six-electron (6e$^-$) oxidation of methanol

$$CH_3OH + H_2O \rightarrow CO_2 + 6H^+ + 6e^- \tag{1}$$

Despite nearly three decades of research and optimization, the best known anode electrocatalysts are a binary Pt-Ru alloy (*21*) and a recently discovered Pt-Ru-Os ternary (*22*). The performance of these alloy catalysts is significantly enhanced relative to Pt alone. The bimetallic alloy is thought to work by a bifunctional or ligand effect mechanism, in which Ru activates water, and Pt activates the methanol C-H bond and also binds the CO intermediate in the reaction (*23, 24*). Although binary alloys of Pt with many other oxophilic elements have been studied, none is more active than high-surface-area Pt-Ru. No predictive model for investigating ternary or quaternary combinations has emerged and, in fact, little is known about the phase equilibria of ternary and quaternary Pt alloys.

Although electrocatalysts are typically tested by measuring current as a function of potential, this approach becomes increasingly unwieldy as the number of samples increases. Successful uses of the combinatorial method—for example, massively parallel screening for biochemical affinity (*1–9*), organic host-guest interactions (*10, 11*), and inorganic phosphorescence (*13*)—often use optical (absorption or emission) detection. Optical detection methods are fast regardless of the complexity of the array, are simple to implement, and allow one to ignore the uninteresting majority of phase space. This method can be adapted to electrochemical screening by recognizing that all half-cell reactions (for example, reaction 1) involve an imbalance of ions. Therefore, a fluorescent indicator that detects the presence or absence of ions (H$^+$ in the case of the DMFC anode) in the diffusion layer images the activity of the array.

This idea is illustrated in a small ternary Pt-Os-Rh array, prepared by manually pipetting appropriate metal salts and aqueous NaBH$_4$ onto Toray carbon paper (Fig. 1). The carbon substrate is electronically conducting but not catalytic for the oxidation of methanol. The array electrode serves as the working electrode in a single-compartment,

T. E. Mallouk, E. Reddington, A. Sapienza, Department of Chemistry, The Pennsylvania State University, University Park, PA 16802, USA.
E. S. Smotkin, B. Gurau, R. Viswanathan, Department of Chemical and Environmental Engineering, Illinois Institute of Technology, Chicago, IL 60616, USA.
S. Sarangapani, ICET, Inc., Norwood, MA 02062, USA.

*To whom correspondence should be addressed. E-mail: chemsmotkin@minna.acc.iit.edu (E.S.S.) or tom@chem.psu.edu (T.E.M.).